A new restriction effect of hard templates for the shrinkage of mesoporous polymer during carbonization†

Mingbo Zheng,[a] Guangbin Ji,[a] Yongwen Wang,[a] Jian Cao,[a] Shaoqing Feng,[a] Lei Liao,[b] Qinglai Du,[a] Lifeng Zhang,[a] Zongxin Ling,[a] Jinsong Liu,[a] Ting Yu,[b] Jieming Cao*[a] and Jie Tao[a]

Received (in Cambridge, UK) 22nd May 2009, Accepted 22nd June 2009
First published as an Advance Article on the web 15th July 2009
DOI: 10.1039/b910128d

A new restriction effect of hard templates for the shrinkage of mesoporous polymer results in anomalous increase of the mesopore size during carbonization.

Mesoporous carbons have generated considerable interest because of their potential applications in catalysis, separation, electrode materials, and gas storage.[1] The nanocasting method has been used extensively in the preparation of mesoporous carbons.[2] However, the pore sizes of mesoporous carbons obtained by this method are always less than 5 nm and the method is costly and fussy.[3] More recently, the organic–organic self-assembly approach has been successfully used to synthesize mesoporous carbons.[4] However, serious shrinkage of polymer during carbonization results in very small mesopore sizes, low pore volumes, and small mesopore surface areas for products. Thus, inhibiting the shrinkage of mesoporous polymer is an effective method to obtain mesoporous carbons with large mesopore sizes, high pore volumes, and large mesopore surface areas.[5]

With the progress of mesoporous carbons, hierarchical mesoporous carbon materials, such as mesoporous carbon nanofiber[6] (MCNF) and mesoporous–macroporous carbon[7] (MMC), have attracted increasing attention because of their interesting structures and properties. Anodic aluminium oxide (AAO) membrane and colloidal crystal are two typical hard templates for the preparation of hierarchical mesoporous materials. Previous studies have demonstrated the nano-confinement effect of these two hard templates for the meso-structure of mesoporous materials.[8] Herein, we report for the first time a new restriction effect of these two hard templates for the shrinkage of mesoporous polymer during carbonization. This novel restriction effect for the shrinkage results in anomalous increase of the mesopore size and the window size of the mesopores during carbonization. Finally, hierarchical MCNF and MMC with very large mesopore sizes, high pore volumes, and large mesopore surface areas were obtained.

[a] *Nanomaterials Research Institute, College of Materials Science and Technology, Nanjing University of Aeronautics and Astronautics, Nanjing 210016, China. E-mail: jmcao@nuaa.edu.cn; Fax: +86-25-84895289*
[b] *Division of Physics and Applied Physics, School of Physical and Mathematical Sciences, Nanyang Technological University, Singapore*

† Electronic supplementary information (ESI) available: Detailed information on the synthesis and characterization of products. See DOI: 10.1039/b910128d

The precursor solution for the AAO template was similar to the F127–resol ethanol solution of FDU-16 (see ESI†).[4b] Several AAO membranes were added into the solution. After ethanol evaporated thoroughly at room temperature, the complex of AAO–F127–resol was taken out and heated at 100 °C for 24 h. The complex was then heat-treated at 350, 500, and 700 °C in N_2, respectively. The corresponding products were denoted as AAO–MPNF-350 (MPNF is the abbreviation for mesoporous polymer nanofiber), AAO–MPNF-500, and AAO–MCNF-700, respectively. For AAO–MPNF-350 and AAO–MCNF-700, AAO templates were removed with 10% aqueous HF. The corresponding products were denoted as MPNF-350 and MCNF-700, respectively. Furthermore, some of MPNF-350 were carbonized at 700 °C in N_2 and the product was denoted as MCNF-350-700.

Fig. 1 shows the BJH pore size distribution curves from adsorption branches for AAO–MPNF-350, AAO–MPNF-500, and AAO–MCNF-700 obtained by using AAO with an average pore diameter of 90 nm as template. The average mesopore sizes for AAO–MPNF-350, AAO–MPNF-500, and AAO–MCNF-700 are about 11, 13.5, and 15 nm, respectively, which indicates that the mesopore size of mesoporous nanofibers (MNFs) increases with increasing heat treatment temperature.

Fig. 2 shows the transmission electron microscopy (TEM) images of MPNF-350 and MCNF-700 obtained by using AAO with an average pore diameter of 90 nm as template. The average mesopore size and the average wall thickness of

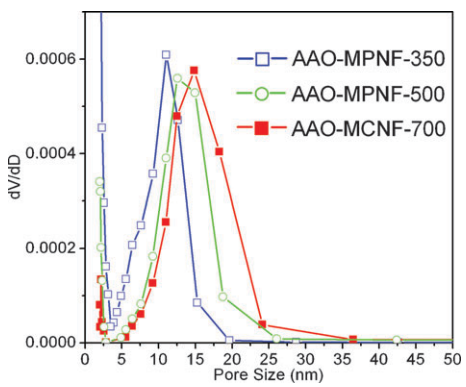

Fig. 1 BJH pore size distribution curves from adsorption branches for AAO–MPNF-350, AAO–MPNF-500, and AAO–MCNF-700 obtained by using AAO with an average pore diameter of 90 nm as template.

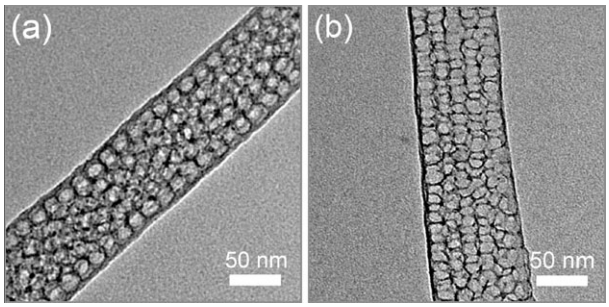

Fig. 2 TEM images of (a) MPNF-350 and (b) MCNF-700 obtained by using AAO with an average pore diameter of 90 nm as template.

MPNF-350 are about 11 and 5 nm, respectively, while the average mesopore size and the average wall thickness of MCNF-700 are about 15 and 2 nm, respectively. These results also indicate that the mesopore size of MNFs increases with increasing heat treatment temperature. (For the scanning electron microscopy (SEM) images, low-magnification TEM images, and Raman spectra of MCNF-700 see Fig. S1–S3, ESI†.)

The N_2 adsorption–desorption isotherms for MCNF-700, MPNF-350, and MCNF-350-700 obtained by using AAO with an average pore diameter of 90 nm as template are shown in Fig. 3a. A typical type-IV curve with a clear capillary condensation step in a relative pressure range of 0.8–0.9 is observed for MCNF-700, implying a uniform mesopore with large pore size. The BJH pore size distribution curves from adsorption branches for the samples are shown in Fig. 3b. The average mesopore sizes of MPNF-350 and MCNF-700 are about 11 and 15 nm, respectively, which indicates that the mesopore sizes of MNFs hardly change after removal of the AAO template. The results also indicate that the mesopore size of MNFs increases with increasing heat treatment temperature. However, the mesopore size of FDU-16 mesoporous materials decreases with increasing heat treatment temperature (the mesopore sizes of FDU-16-350 and FDU-16-700 were 6.6 and 3.8 nm, respectively).[4b] The BJH pore size distribution curves from desorption branches (Fig. S4, ESI†) show that the window size of the mesopores of MCNF-700 is also obviously larger than that of MPNF-350, which indicates that the

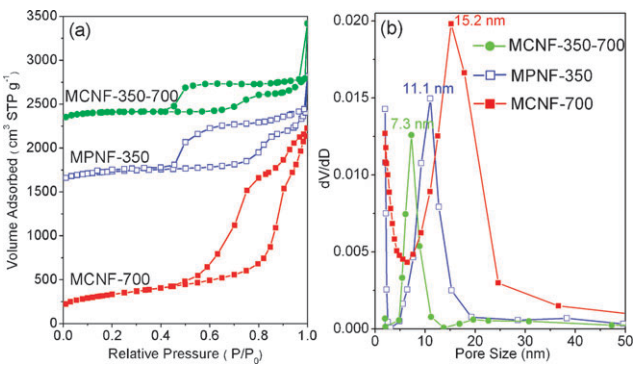

Fig. 3 (a) N_2 adsorption–desorption isotherms and (b) BJH pore size distribution curves from adsorption branches of MCNF-700, MPNF-350, and MCNF-350-700 obtained by using AAO with an average pore diameter of 90 nm as template. The isotherms of MPNF-350 and MCNF-350-700 are offset vertically by 1500 and 2000 $cm^3\ g^{-1}$, respectively.

window size of the mesopores also increases during carbonization. The Brunauer–Emmett–Teller (BET) surface area and the pore volume for MCNF-700 are estimated to be 1154 $m^2\ g^{-1}$ and 3.44 $cm^3\ g^{-1}$, respectively, which are much larger than those of FDU-16-700. Due to its thin mesopore wall, very large mesopore size, and the stacking of MCNFs, MCNF-700 has such a large pore volume. The micropore area and the micropore volume of MCNF-700 are only 246 $m^2\ g^{-1}$ and 0.12 $cm^3\ g^{-1}$, respectively. These results indicate that most of the BET surface area and the pore volume of MCNF-700 are from the mesopores, which is different from FDU-16-700.

MNFs were also synthesized by using AAO templates with average pore diameters of 50, 200, and 300 nm, respectively. The results of N_2 adsorption–desorption analysis (Table S1 and Fig. S7, S10, S12, ESI†) indicate that the mesopore size of MNFs increases with increasing heat treatment temperature. Furthermore, the increment of mesopore size from 350 to 700 °C for MNFs (Table S1, ESI†) decreases with increasing pore diameter of AAO template. (For the SEM and TEM images of MNFs see Fig. S5, S6, S8, S9, S11, ESI†.)

The restriction effect of the AAO template for the shrinkage of mesoporous polymer is illustrated in Fig. 4. The nanopores of AAO were completely filled with F127–resol mixture after the ethanol evaporated. After heat treatment at 100 °C for 24 h, the resol transformed into a rigid polymer network around the F127 micelle by thermopolymerization.[4a,b] There was an interaction between the resin polymer and the interior surface of AAO, since they both have a large number of hydroxyl groups.[6f,9] The F127 template was removed after heat treatment at 350 °C in N_2. During the heat treatment process, for FDU-16, the resin polymer shrank continuously.[4b] However, the resin polymer nanofiber within the nanopore of AAO could not shrink freely because of the strong interaction between the polymer and the alumina.[6f] Although nanofibers could not shrink integrally, shrinkage still existed in the interior of the nanofibers. The mesopore wall of the nanofibers shrank continuously with increasing temperature. Thus, the thickness of the mesopore wall decreased and the mesopore size increased continuously with increasing temperature. Meanwhile, the window of the mesopores was also enlarged continuously. The plan-view TEM image (see Fig. S13, ESI†) of AAO–MCNF-700 indicates that the surface of MCNF-700 still connects tightly with the pore wall of AAO after carbonization at 700 °C, which proves the interaction between the MNFs and the pore surface of AAO during carbonization.

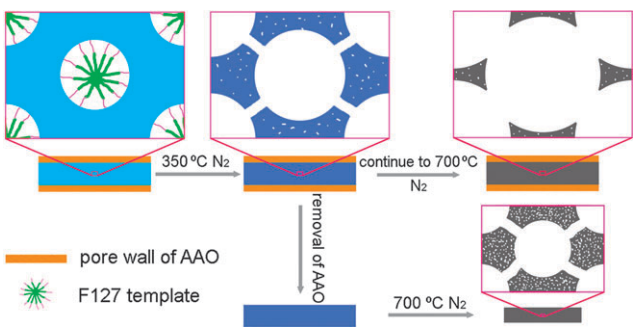

Fig. 4 Schematic illustration of the restriction effect of AAO for the shrinkage of mesoporous polymer during carbonization.

The increment of mesopore size from 350 to 700 °C for MNFs decreases with increasing pore diameter of AAO template, which indicates that the restriction effect for the shrinkage weakens with increasing pore diameter of AAO. When MPNF-350 was carbonized at 700 °C, it shrank freely due to the disappearance of the restriction effect and its mesopore size decreased accordingly (Fig. 3b). In addition, in our previous work, MCNFs with core–shell structure were obtained by using the F127–resol ethanol solution of FDU-15 as the precursor solution.[6f] The formation of the core–shell structure is also due to the restriction effect of the AAO template.

SiO_2 colloidal crystal self-assembled by SiO_2 microspheres was also used as the hard template because it had nanoscale-space between the SiO_2 microspheres. The precursor solution for SiO_2 colloidal crystal was similar to the F127–resol ethanol solution of FDU-15.[4b] The complex of SiO_2–F127–resol was heat-treated at 350, 700, and 900 °C in N_2, respectively. After removal of the SiO_2 template, the corresponding products were denoted as MMP-350 (MMP is the abbreviation for mesoporous–macroporous polymer), MMC-700, and MMC-900, respectively (for the detailed preparations of MMP and MMC see ESI†). The results of N_2 adsorption–desorption analysis (Fig. 5) show that the mesopore size of MMC-700 is larger than that of MMP-350, which indicates that the restriction effect for the shrinkage also exists in the nanoscale-space of the SiO_2 colloidal crystal. The average mesopore size of MMC-700 is about 14.8 nm, which is much larger than 3.2 nm of FDU-15-700. The BET surface area and the pore volume of MMC-700 are estimated to be 1243 $m^2\ g^{-1}$ and 3.49 $cm^3\ g^{-1}$, respectively, which are also much larger than those of FDU-15-700. Furthermore, the micropore area and the micropore volume of MMC-700 are only 333 $m^2\ g^{-1}$ and 0.16 $cm^3\ g^{-1}$, respectively. In addition, the mesopore size of MMC-900 (Table S1, ESI†) is almost the same as that of MMC-700, which indicates that the shrinkage is very slight from 700 to 900 °C (for the SEM and TEM images of MMC-700 see Fig. S14, ESI†).

In summary, the carbonization process of mesoporous polymer within the nanoscale-space of the hard templates is different from that under unrestricted conditions due to a new restriction effect. This novel restriction effect results in anomalous increase of the mesopore size and the window size of the mesopores during carbonization and provides a new approach for the synthesis of mesoporous carbons with large mesopore sizes, high pore volumes, and large mesopore surface areas. Furthermore, this restriction effect may be applicable to other mesoporous materials which are prone to shrink during the heat treatment and to other hard templates with nanoscale-space.

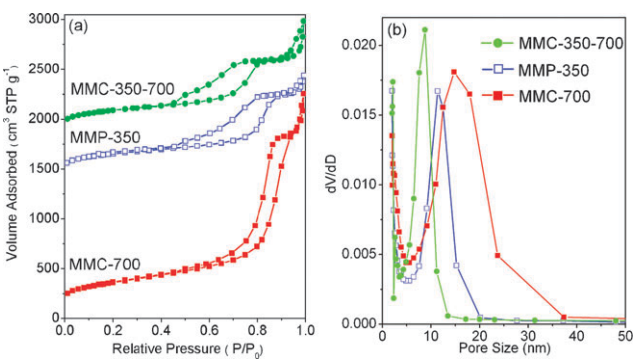

Fig. 5 (a) N_2 adsorption–desorption isotherms and (b) BJH pore size distribution curves from adsorption branches for MMC-700, MMP-350, and MMC-350-700 (obtained by carbonizing MMP-350 at 700 °C in N_2). The isotherms of MMP-350 and MMC-350-700 are offset vertically by 1400 and 1700 $cm^3\ g^{-1}$, respectively.

We thank Prof. Dong-yuan Zhao of Fudan University for advice and Prof. Jian-bo Wang and Dr Lei Jin of Wuhan University for assistance. This work was supported by Doctor Innovation Funds of Jiangsu Province (xm06-57), National Natural Science Foundation of China (50502020, 50701024), Natural Science Foundation of Jiangsu Province (BK2006195).

Notes and references

1 (*a*) S. H. Joo, S. J. Choi, I. Oh, J. Kwak, Z. Liu, O. Terasaki and R. Ryoo, *Nature*, 2001, **412**, 169; (*b*) J. S. Yu, S. Kang, S. B. Yoon and G. Chai, *J. Am. Chem. Soc.*, 2002, **124**, 9382; (*c*) A. Lu, W. Schmidt, N. Matoussevitch, H. Bönnemann, B. Spliethoff, B. Tesche, E. Bill, W. Kiefer and F. Schüth, *Angew. Chem., Int. Ed.*, 2004, **43**, 4303; (*d*) J. Lee, J. Kim and T. Hyeon, *Adv. Mater.*, 2006, **18**, 2073.

2 R. Ryoo, S. H. Joo and S. Jun, *J. Phys. Chem. B*, 1999, **103**, 7743.

3 (*a*) Y. Deng, T. Yu, Y. Wan, Y. Shi, Y. Meng, D. Gu, L. Zhang, Y. Huang, C. Liu, X. Wu and D. Zhao, *J. Am. Chem. Soc.*, 2007, **129**, 1690; (*b*) Y. Deng, C. Liu, D. Gu, T. Yu, B. Tu and D. Zhao, *J. Mater. Chem.*, 2008, **18**, 91.

4 (*a*) Y. Meng, D. Gu, F. Zhang, Y. Shi, H. Yang, Z. Li, C. Yu, B. Tu and D. Zhao, *Angew. Chem., Int. Ed.*, 2005, **44**, 7053; (*b*) Y. Meng, D. Gu, F. Zhang, Y. Shi, L. Cheng, D. Feng, Z. Wu, Z. Chen, Y. Wan, A. Stein and D. Zhao, *Chem. Mater.*, 2006, **18**, 4447; (*c*) S. Tanaka, N. Nishiyama, Y. Egashira and K. Ueyama, *Chem. Commun.*, 2005, 2125; (*d*) C. Liang and S. Dai, *J. Am. Chem. Soc.*, 2006, **128**, 5316.

5 R. Liu, Y. Shi, Y. Wan, Y. Meng, F. Zhang, D. Gu, Z. Chen, B. Tu and D. Zhao, *J. Am. Chem. Soc.*, 2006, **128**, 11652.

6 (*a*) D. J. Cott, N. Petkov, M. A. Morris, B. Platschek, T. Bein and J. D. Holmes, *J. Am. Chem. Soc.*, 2006, **128**, 3920; (*b*) A. T. Rodriguez, M. Chen, Z. Chen, C. J. Brinker and H. Fan, *J. Am. Chem. Soc.*, 2006, **128**, 9276; (*c*) W. Chae, M. An, S. Lee, M. Son, K. Yoo and Y. Kim, *J. Phys. Chem. B*, 2006, **110**, 6447; (*d*) K. Wang, W. Zhang, R. Phelan, M. A. Morris and J. D. Holmes, *J. Am. Chem. Soc.*, 2007, **129**, 13388; (*e*) M. Steinhart, C. Liang, G. W. Lynn, U. Gösele and S. Dai, *Chem. Mater.*, 2007, **19**, 2383; (*f*) M. B. Zheng, J. M. Cao, X. F. Ke, G. B. Ji, Y. P. Chen, K. Shen and J. Tao, *Carbon*, 2007, **45**, 1111; (*g*) K. Wang, P. Birjukovs, D. Erts, R. Phelan, M. A. Morris, H. Zhou and J. D. Holmes, *J. Mater. Chem.*, 2009, **19**, 1331; (*h*) L. Liao, M. B. Zheng, Z. Zhang, B. Yan, X. F. Chang, G. B. Ji, Z. X. Shen, T. Wu, J. M. Cao, J. X. Zhang, H. Gong, J. Cao and T. Yu, *Carbon*, 2009, **47**, 1841; (*i*) Y. Liang, X. Feng, L. Zhi, U. Kolb and K. Müllen, *Chem. Commun.*, 2009, 809.

7 (*a*) G. S. Chai, I. S. Shin and J. S. Yu, *Adv. Mater.*, 2004, **16**, 2057; (*b*) Z. Wang, F. Li, N. S. Ergang and A. Stein, *Chem. Mater.*, 2006, **18**, 5543; (*c*) Y. Deng, C. Liu, T. Yu, F. Liu, F. Zhang, Y. Wan, L. Zhang, C. Wang, B. Tu, P. A. Webley, H. Wang and D. Zhao, *Chem. Mater.*, 2007, **19**, 3271.

8 (*a*) Y. Wu, G. Cheng, K. Katsov, S. W. Sides, J. Wang, J. Tang, G. H. Fredrickson, M. Moskovits and G. D. Stucky, *Nat. Mater.*, 2004, **3**, 816; (*b*) D. Wang, R. Kou, Z. Yang, J. He, Z. Yang and Y. Lu, *Chem. Commun.*, 2005, 166; (*c*) B. Platschek, N. Petkov and T. Bein, *Angew. Chem., Int. Ed.*, 2006, **45**, 1134; (*d*) A. Y. Ku, S. T. Taylor and S. M. Loureiro, *J. Am. Chem. Soc.*, 2005, **127**, 6934; (*e*) F. Li, Z. Wang, N. S. Ergang, C. A. Fyfe and A. Stein, *Langmuir*, 2007, **23**, 3996.

9 (*a*) M. R. Alexander, G. Beamson, P. Bailey, T. C. Q. Noakes, P. Skeldon and G. E. Thompson, *Surf. Interface Anal.*, 2003, **35**, 649; (*b*) J. Jang and J. Bae, *Adv. Funct. Mater.*, 2005, **15**, 1877.